Study of Class-D Power Amplifiers for Underwater Acoustic OFDM Transmissions

Xiaoka Xu*, Shengli Zhou*, Kaleel Mahmood*, Li Wei†, and Jun-Hong Cui†
*Department of Electrical and Computer Engineering, University of Connecticut, Storrs, CT 06269
†Department of Computer Science and Engineering, University of Connecticut, Storrs, CT 06269

***Abstract*—In this paper, we investigate the power amplifier design for underwater acoustic OFDM systems. Using the pilot signal to noise ratio (PSNR) of an OFDM signal as the design criterion, we study the impact of the modulation frequency and the number of quantization bits for the class-D power amplifiers. Experimental results show that there is PSNR performance ceiling as the number of quantization bits increases.**

I. Introduction

In the past decade, OFDM technology has been successfully developed for high-data-rate underwater acoustic communications. The research of point-to-point communication has been maturing, as a result the research focus has been shifting to modem system design [1]–[3]. Power amplification is the one important component for modem design.

Class D power amplifiers are the primary choice for underwater acoustic communications due to the following reasons:

- *High power conversion efficiency*. Compared with linear power amplifiers (class-A, class-B, class-AB), class-D power amplifiers have much higher efficiency, typically more than 90%. High efficiency is extremely important in underwater environments because the battery life is limited. Because of high efficiency of a class-D power amplifier, power waste on dissipation will be reduced and hence small heatsink can be used, which can lead to a compact power amplifier circuit board to be placed inside the modem housing.
- *Linearity acceptance*. With enough quantization bits and modulation frequency, the linearity of the class-D power amplifier will be acceptable. If the linearity of transmitted signal, which is measured by pilot signal to noise ratio (PSNR) of an OFDM signal in this paper, is above a certain value, higher linearity will not lead to higher PSNR at the received side due to the ambient noise and the channel-induced distortions.
- *Fully digital modulator*. Compared with class-A and class-AB power amplifiers, another advantage of class D power amplifiers is that their input signal, the pulse-width modulation (PWM) waveform, can be directly generated by digital computation.

From the power amplifier design perspective, the PWM modulation frequency and the number of quantization bits are the two most important parameters, which will decide the linearity of class-D power amplifiers. In this work, we setup the testbed and use experimental results to evaluate the performance of the class-D power amplifiers regarding to different modulation frequencies and numbers of quantization bits. Theoretical study of PWM can be found in e.g., [4].

The rest of this paper is organized as follows. The system model and the criterion of power amplifier design are described in Section II. Section III presents the numerical results and Section IV draws the conclusions.

II. System Model and Design Criterion

A. Transmitted OFDM Signal

Let T_s denote the signal duration and T_g the zero padding interval. The OFDM block duration is $T_{\rm bl} = T_s + T_g$. The kth subcarrier is at frequency

$$f_k = f_c + k/T_s, \qquad k = -K/2, \cdots, K/2-1, \qquad (1)$$

where f_c is the carrier frequency and K subcarriers are used so that the bandwidth is $B = K/T_s$. Let $s[k]$ denote the information symbol to be transmitted on the kth subcarrier and $\mathcal{S}_{\rm all} = \mathcal{S}_{\rm D} \bigcup \mathcal{S}_{\rm P} \bigcup \mathcal{S}_{\rm N} = \{-K/2, \cdots, K/2-1\}$ the set of all subcarriers, where $\mathcal{S}_{\rm D}$, $\mathcal{S}_{\rm P}$ and $\mathcal{S}_{\rm N}$ are the sets of data, pilot and null subcarriers, respectively.

The transmitted signal in the passband is given by

$$\tilde{x}(t) = 2\mathrm{Re}\left\{ \left[\sum_{k\in\mathcal{S}_{\rm all}} s[k] e^{j2\pi \frac{k}{T} t} g(t) \right] e^{j2\pi f_c t} \right\}, \quad t \in [0, T_{\rm bl}]. \qquad (2)$$

where $g(t)$ is a pulse-shaping window. For a rectangular window

$$g(t) = \begin{cases} 1/T_s, & t \in [0, T_s] \\ 0, & \text{otherwise}, \end{cases} \qquad (3)$$

Other pulse shapers, such as raised cosine window, can be applied as well.

B. PWM Modulation Model

The transmitted signal $\tilde{x}(t)$ is first modulated to a PWM waveform. The PWM modulation process can be seen in Fig. 1, where two types of PWM modulations, natural sampling PWM (NPWM) and uniform sampling PWM (UPWM) are illustrated. NPWM uses a comparison waveform to sample the original signal, wherever the comparison waveform crosses the original signal a sample value is recorded and translated into a pulse duration on the PWM wave. Two types of comparison waves are generally used in NPWM, either a saw tooth waveform in which case the PWM is known as single

978-0-933957-40-4

edge NPWM, or a triangle waveform is used which is known as double edge NPWM. Instead of using crossing points, the pulse durations of UPWM are only decided by digital samplers in a fixed sampling rate, and it can be implemented by setting the registers of PWM controller in microcontroller (MCU) or digital signal processor (DSP) straightforwardly. Only UPWM is implemented for OFDM systems in this paper.

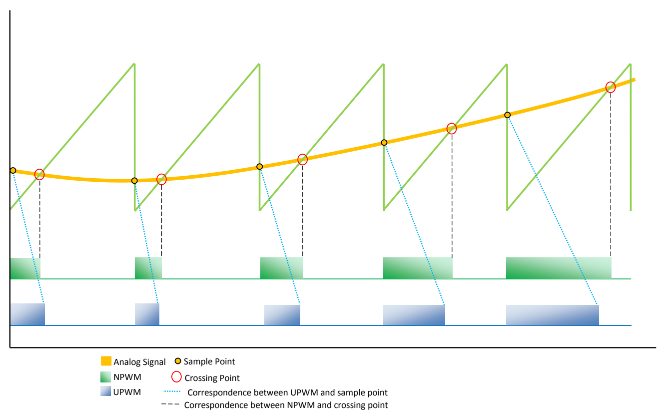

Fig. 1. Difference between UPWM and NPWM [4]

After getting the UPWM waveform, it is amplified by a switch power stage using the metal-oxide-semiconductor field-effect transistor (MOSFET). The amplified UPWM waveform passes through a low pass filter, and the amplified analog signal can be obtained from the class-D power amplifier. In order to deliver more power, the matching circuit is needed to match the impedance difference between the transducer and the class-D power amplifier. The whole procedure of amplifications for OFDM signals can be seen in Fig. 2, where we split the PWM modulation in two components. The class-D power amplifier is composed by three modules: PWM modulation, switch power stage and low pass filter.

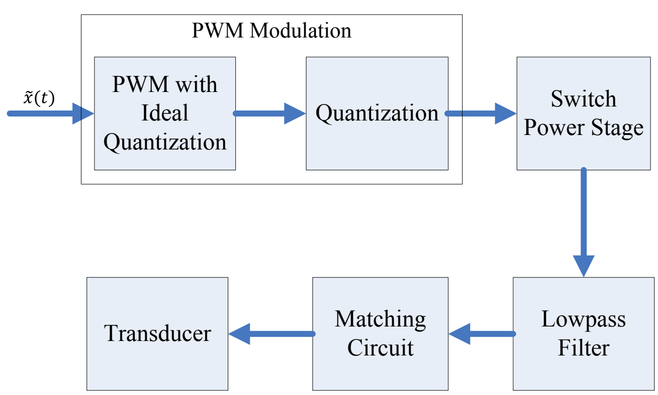

Fig. 2. Amplifications of OFDM signals

C. Criterion of Power Amplifier Design

The receiver performs the following three steps to obtain the frequency-domain samples from the passband signal shown in Fig. 3.

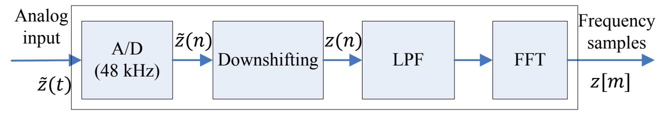

Fig. 3. PSNR measurement

- The passband signal $\tilde{z}(t)$ is sampled in passband to digital samplings $\tilde{z}[n]$ based on sampling rate F_s. We use $F_s =$ 48 kHz in this paper.
- The passband digital signal $\tilde{z}[n]$ is shifted to baseband $z[n] = \text{LPF}\left(\tilde{z}(n)e^{-j2\pi f_c n/F_s}\right)$, where LPF$(\cdot)$ stands for low pass filtering.
- The sample on the mth subcarrier is obtained as

$$\bar{z}[m] = \sum_{n=1}^{\lfloor T_{\text{bl}} \cdot F_s \rfloor} z[n] e^{-j2\pi \frac{m}{T} n/F_s}. \quad (4)$$

where $\lfloor \cdot \rfloor$ is the floor function.

The samples on all the subcarriers are obtained simultaneously by an FFT operation.

In this paper, we use the PSNR of the transmitted signal as the design criterion. For each OFDM symbol, the pilot PSNR is computed as

$$\text{PSNR} = \frac{\text{E}_{m \in \mathcal{S}_\text{P}} \left\{ |\bar{z}[m]|^2 \right\} - \text{E}_{m \in \mathcal{S}_\text{N}} \left\{ |\bar{z}[m]|^2 \right\}}{\text{E}_{m \in \mathcal{S}_\text{N}} \left\{ |\bar{z}[m]|^2 \right\}} \quad (5)$$

where $\mathcal{S}_\text{P}$ and $\mathcal{S}_\text{N}$ are the non-overlapping sets of pilot subcarriers and null subcarriers respectively. Note that the out-of-band noise is not used in our calculations as it will be filtered out by the bandpass filter at the receiver. The variance of the inband noise as measured on the null subcarriers is a good indicator of the intercarrier interference due to amplifier distortions. The PSNR at the receiver side is smaller than that at the transmitter side due to channel attenuations and the ambient noise.

III. Numerical Results

The OFDM system parameters of the experimental tests are: system bandwidth B = 6 kHz, center frequency f_c = 17 kHz, K = 1024 subcarriers, the duration of one OFDM symbol T = K/B = 170.7 ms, and the guard interval T_g = 50 ms. Among the K = 1024 subcarriers, there are K_n = 96 null subcarriers and K_p = 256 pilot subcarriers, and K_d = 672 data subcarriers.

A. Trade-off Between Modulation Frequency and Quantization Bits

Focus on the fully digital processing class-D power amplifiers except the low-pass filter to recover the analog signal from the digital signal, two of the key parameters are the modulation frequency and the number of quantization bits. For specified DSP/MCU, the PWM duty cycle can only be specified with a finite resolution, which depends on the system clock frequency and the PWM modulation frequency. There is trade-off between the modulation frequency and the number of quantization bits. The higher modulation frequency is, the smaller distortion will be from the PWM modulation, while for each cycle of PWM signal, the extra bits used to specify the width of PWM will be smaller and more quantization noise will be induced. The relationship between the maximum number of quantization bits γ and the modulation frequency F_{PWM} can be seen in (6).

$$\gamma = \log_2 \left(\frac{F_{\mathrm{BC}}}{F_{\mathrm{PWM}}} \right) \tag{6}$$

where F_{BC} is the base clock of PWM modulator.

In the tests we set the core clock as 294.912 MHz and the base clock of the PWM modulator as F_{BC} = 147.456 MHz. The relationship between the maximum number of quantization bits and the UPWM modulation frequency is shown as

F_{PWM} (kHz)	96	144	288	384	576
γ (bit)	10.59	10	9	8.59	8

from which we can see that the higher modulation frequency is, the less number of quantization bits can be used.

B. Experimental Setup and Results

Figure 4 shows the experimental setup used to generate the PWM waveforms and test the performance of power amplifier design. First an OMAP-L137 digital signal processing evaluation board is used to produce the UPWM modulated waveform. This waveform is sent to the TAS5612PHD2EVM, which consists of the power stage and low pass filter, to be amplified. The TAS5612PHD2EVM power amplifier is monitored and controlled by a USB control board and is powered by 30 volt power supply. Once the signal is amplified by the power amplifier it is then attenuated by using a transformer and resistor network configuration before finally being passed to a lab modem [2], which uses OMAP-L137 as the processor.

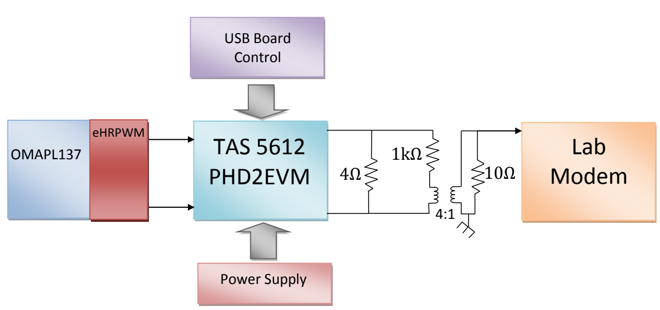

Fig. 4. Experimental setup

There are two modes in OMP-L137 PWM module called enhanced high-resolution pulse-width modulator (eHRPWM) and conventional pulse-width modulator (cPWM). Only the cPWM is investigated in the experimental results. By setting the modulation frequency as 576 kHz, 384 kHz, 288 kHz, 144 kHZ, and 96 kHz, we get the PSNR performance of different modulation frequency and quantization bits in Fig. 5. Our observations from Fig. 5 are as follows.

- Along the same modulation frequency, the more quantization bits are used, the higher the PSNR gets.
- With the same number of quantization bits, higher modulation frequency leads to higher PSNR.
- There is a PSNR ceiling for quantization around 47 dB. When the PSNR reaches to 47 dB, more quantization bits will not lead to higher PSNR.
- When the modulation frequency is less than 288 kHz, which is roughly 15 times of the highest frequency 20 kHz, the increase of modulation frequency will lead to higher PSNR performance. While when the modulation frequency is more than 288 kHz, the increase of modulation frequency can only slightly increase the PSNR performance.

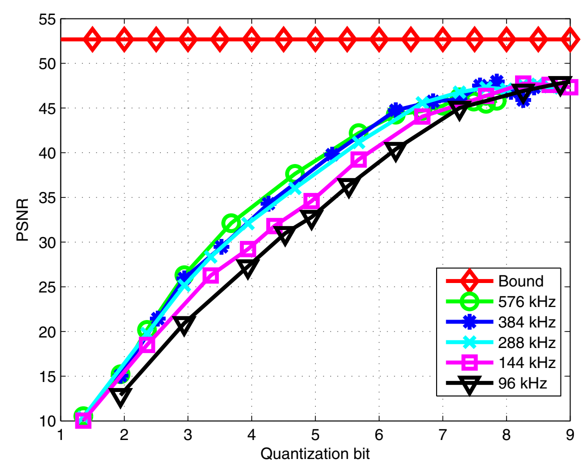

Fig. 5. Experimental results, where the bound is computed based on an ideal power amplifier

IV. Conclusions

In this paper, we studied underwater acoustic OFDM from the power amplifier design perspective. By using the PSNR as the design criterion, we investigated the performance of class-D power amplifiers regarding to different modulation frequencies and numbers of quantization bits. Experimental results showed that there were PSNR performance ceiling as the number of quantization bits increases.

References

[1] E. Gallimore, J. Partan, I. Vaughn, S. Singh, J. Shusta, and L. Freitag, "The WHOI micromodem-2: A scalable system for acoustic communications and networking," in *Proc. of OCEANS Conf.*, Sep. 2010.

[2] H. Yan, L. Wan, S. Zhou, Z. Shi, J.-H. Cui, J. Huang, and H. Zhou, "DSP based receiver implementation for OFDM acoustic modems," *Elsevier Journal on Physical Communication*, vol. 5, no. 1, pp. 22–32, Mar. 2012.

[3] M. Chitre and I. Topor and T.-B. Koay, "The UNET-2 modem - an extensible tool for underwater networking research," *Proceedings of IEEE OCEANS*, Yeosu, Korea, May 2012.

[4] C. Pascual, Z. Song, P. T. Krein, D. V. Sarwate, P. Midya, and W. B. J. Roeckner, "High-fidelity PWM inverter for digital audio amplification: Spectral analysis, real-time DSP implementation, and results," *IEEE Trans. on Power Electronics*, vol. 18, no. 1, pp. 473–485, Jan 2003.